BIOCHEMISTRY
including biophysical chemistry & molecular biology
Article

Biochemistry **2009,** *48,* 12283–12289 12283
DOI: 10.1021/bi901657b

Microsecond Time-Resolved Circular Dichroism of Rhodopsin Photointermediates[†]

Yiren Gu Thomas, Istvan Szundi, James W. Lewis, and David S. Kliger*

Department of Chemistry and Biochemistry, University of California, Santa Cruz, California 95064

Received September 22, 2009; Revised Manuscript Received November 10, 2009

ABSTRACT: Time-resolved circular dichroism measurements, over a spectral range from 300 to 700 nm, were made at delays of 5, 100, and 500 μs after room-temperature photoexcitation of bovine rhodopsin in a lauryl maltoside suspension. The purpose was to provide more structural information about intermediate states in the activation of rhodopsin and other G protein-coupled receptors. In particular, information was sought about photointermediates that are isochromic or nearly isochromic in their unpolarized absorbance. The circular dichroism spectrum of lumirhodopsin, obtained after correcting the 5 μs difference CD data for the bleached rhodopsin, was in reasonable agreement with the lumirhodopsin CD spectrum obtained previously by thermal trapping at −76 °C. Similarly, the metarhodopsin II spectrum obtained with a 500 μs delay was also in agreement with the results of previous work on the temperature-trapped form of metarhodopsin II. However, the CD of the mixture formed with a 100 μs delay after photoexcitation, whose only visible absorbing component is lumirhodopsin, could not be accounted for near 480 nm in terms of the initially formed, 5 μs lumirhodopsin CD spectrum. Thus, the CD spectrum of lumirhodopsin changes on the time scale from 5 to 100 μs, showing reduced rotational strength in its visible band, possibly associated with either a process responsible for a small spectral shift that occurs in the lumirhodopsin absorbance spectrum at earlier times or the Schiff base deprotonation−reprotonation which occurs during equilibration of lumirhodopsin with the Meta I_{380} photointermediate. Either explanation suggests a chromophore conformation change closely associated with deprotonation which could be the earliest direct trigger of activation.

The X-ray crystal structure of rhodopsin provides a fundamental basis for any model of visual pigment activation. However, the X-ray structure of rhodopsin, while rich in three-dimensional structural information, lacks a time coordinate, making that picture just the beginning of a yet to be constructed motion picture. Based on the initial coordinates, a detailed series of activation steps remains to be elucidated, and those cannot be adapted from another system, since a heptahelical membrane-bound protein triggered by isomerization of its *N*-retinylidene Schiff base chromophore is essentially unprecedented. What is needed to fill in the activation mechanism blanks are dynamic measurements, especially those with structural content, conducted at sufficiently early times that they can be interpreted in terms of small perturbations of the initial crystal structure data.

Traditionally, UV−visible absorbance measurements have the highest time resolution of any technique by several orders of magnitude. As a light-activated protein, rhodopsin exposes more of its activation steps for optical study than do most protein systems. Given the wide time range accessible to UV−visible absorbance measurement, it is not surprising that they reveal a complicated series of intermediate steps in visual pigment activation (see Scheme 1). While not simple, those processes are important, with significance beyond retinal health since they have potential relevance to other members of the important G protein-coupled receptor (GPCR)[1] family. Thus, rhodopsin can serve as a platform for the development of a broader model of GPCR activation, a model potentially useful for better control of many popular medicinal targets. However, a practical picture, particularly of the temporally complex rhodopsin activation mechanism, turns out to require more information than simple absorbance changes provide.

Spectral changes provide the most basic structural information about rhodopsin photoactivation. The earliest red-shifted photointermediate's spectrum reflects chromophore torsion (*4*, *5*), and a subsequent blue-shifted photointermediate is believed to result from limited torsional relaxation (*6*). Much later, deprotonation of the retinylidene Schiff base (SB) is signaled by the shift in photoproduct absorption maximum from ∼480 to 380 nm. However, extensive study of rhodopsin photointermediates has revealed not just one but several species with similar 380 nm absorption (*7*−*9*), leaving much structural detail to be resolved by other techniques. Some of the 380 nm absorbing forms are sufficiently stable that slow techniques can be applied to their study, but one 380 nm absorbing form, Meta I_{380}, which precedes the G protein-activating photointermediate, Meta II, has a submillisecond lifetime at near-physiological temperatures and has not been well-characterized at temperatures significantly below that. Since more information about events immediately preceding activation near physiological temperature is needed, here we use time-resolved circular dichroism (TRCD) on the microsecond time scale to study rhodopsin's photointermediates.

[†]This research was supported by Grant EY00983 from the National Eye Institute of the National Institutes of Health.

*To whom correspondence should be addressed. Phone: (831) 459-2106. Fax: (831) 459-4161. E-mail: kliger@chemistry.ucsc.edu.

[1]Abbreviations: Batho, bathorhodopsin; BSI, blue-shifted intermediate; CHAPS, 3-[(3-cholamidopropyl)dimethylammonio]-1-propanesulfonate; CD, circular dichroism; GPCR, G protein-coupled receptor; ICCD, intensified charge-coupled device; LM, lauryl maltoside; Lumi, lumirhodopsin; Meta, metarhodopsin; ORD, optical rotatory dispersion; ROS, rod outer segments; SB, *N*-retinylidene Schiff base; TBS, Tris-buffered saline; TRCD, time-resolved circular dichroism.

Published on Web 11/11/2009

Scheme 1: Rhodopsin Photointermediate Sequence near Physiological Temperatures[a]

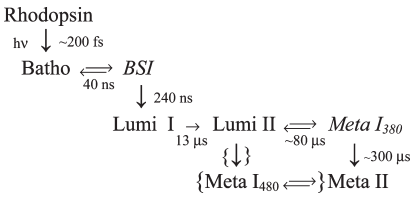

[a]Some of the intermediates appearing above can be trapped after low-temperature photolysis, but those shown in italics only build up appreciable concentrations near physiological temperatures (*1*−*3*). The time constants given are appropriate for lauryl maltoside (LM) suspensions of rhodopsin near 20 °C. This general scheme also holds for membrane samples with the same time constants up to Lumi II formation. Braces enclose portions of the scheme that occur at low temperatures in membrane but do not take place significantly in LM. This scheme is simplified in that a single Meta II product is shown. This neglects proton uptake that occurs between two isochromic forms of Meta II to produce the G protein-activating form.

Although strong linear birefringence transients due to molecular rotation (*10*) prevent TRCD measurement in the native membrane environment, Meta I_{380} can be observed after rhodopsin photolysis in lauryl maltoside detergent suspensions. Since molecular rotation is much faster in such suspensions, linear birefringence transients have relaxed before Meta I_{380} appears, which allows TRCD study on the microsecond time scale.

MATERIALS AND METHODS

Rhodopsin Sample Preparation. Dark-adapted, frozen bovine retinas, dissected into 0.5 mL per retina 43% sucrose in TBS [10 mM Tris, 30 mM NaCl, 60 mM KCl, 2 mM $MgCl_2$, and 0.1 mM EDTA (pH 7)], were purchased from J. A. Lawson (Omaha, NE). Rod outer segments (ROS) were prepared as previously described (*9*). To remove the extrinsic membrane proteins, the ROS were pelleted (20 min) and washed via three cycles of centrifugation, twice with 1 mM EDTA (pH 7.0) (45 min each), and once with TBS (all the centrifugations were conducted at 17000 rpm and ~10 °C, using a Sorvall model SS-34 rotor). After the final wash, membrane disks were resuspended in TBS at a rhodopsin concentration of ~2 mg/mL and frozen until the day of their use in CD measurements.

Approximately 2 h before circular dichroism measurements, TBS-suspended frozen membrane disks were thawed and pelleted by centrifugation at 17K rpm and ~10 °C for 15 min. The pellet was then dissolved in 4% lauryl maltoside (LM, Anatrace, analytical grade) followed by centrifugation at 17K rpm and ~18 °C for 15 min to yield a clear rhodopsin solution. The final rhodopsin concentration was 1.6−2.0 mg/mL. The rhodopsin concentration was determined, after 1:10 dilution in 3% Ammonyx in TBS, by using a Shimadzu UV-2101PC spectrophotometer.

Time-Resolved Circular Dichroism Measurements. To investigate chiral structure differences in the Lumi, Meta I_{380}, and Meta II photointermediates, we chose to measure CD spectra at three time delays following laser photoexcitation, 5 μs (when only freshly formed Lumi is present), 100 μs (when an equilibrated mixture containing approximately equal amounts of Lumi and Meta I_{380} is present), and 500 μs (when only Meta II is present). An ellipsometric, time-resolved circular dichroism (TRCD) technique was used to measure the CD of the rhodopsin solutions both before and after photoexcitation by a pulse of laser light at room temperature. Figure 1 shows a diagram of the apparatus. At any desired time delay after photoexcitation, the gated array detector (7 μs gate) measured the excess of either right or left circularly polarized light in the elliptically polarized probe beam over an ~400 nm range of wavelengths. The TRCD apparatus used here is similar to the one described previously (*11*), except that a pair of 3 in. focal length lenses were placed between the polarizer and analyzer, to focus the polarized probe light on the sample volume and recollimate it again prior to analysis, to improve the signal-to-noise ratio of the CD signal. Standard fused silica lenses were suitable for this purpose, but the best results were obtained after those lenses were rotated around the optical axis of the apparatus (primarily to reduce the intensity passed with crossed polarizers and secondarily to reduce offsets of the CD baseline with water in the cell). A 2 mm path length flow cell was constructed with replaceable windows to allow selection of the least strained windows, which were very thin (0.2 mm) fused silica or glass disks. Rhodopsin samples were excited using a 7 ns pulse of 477 nm light (fluence of ~100 $\mu J/mm^2$) from either an Opotek Vibrant VIS 2 laser optical parametric oscillator system or a dye laser system described previously (*9*). Samples were replenished for each measurement by pumping ~32 μL of solution (approximately twice the irradiated volume) before the next photolysis occurred. The vertically polarized laser pulse entered the sample at a crossing angle of approximately 25° relative to the probe beam propagation direction. Care needed to be taken to reduce laser pulse-to-pulse energy variation since the intensities transmitted for right and left elliptically polarized probe pulses were measured using different laser pulses (and rhodopsin samples). If significant variation in photoexcitation were to occur between measurements taken with the two ellipticities, CD results would be contaminated by significant noise due to the difference in absorbance changes. Although like other sources of noise this source will average out, it was important to minimize it by carefully optimizing laser operation by using a pyroelectric Joule meter to monitor pulse-to-pulse variation before commencing CD work on rhodopsin.

Time-Resolved Absorbance Measurements. To convert the time-resolved CD data into absolute CD spectra of photointermediates, we had to determine the composition of the sample at the measured delay times. This was done using the same data that were used for CD but combined in a different way. Absorbance difference spectra were obtained from the sum of the ellipse short axis data rather than the difference that was used for CD measurement.

Static Circular Dichroism of Rhodopsin in Lauryl Maltoside. The circular dichroism of rhodopsin suspensions in 4% LM was measured without photoexcitation using both a conventional Aviv 60 CD instrument and the TRCD apparatus. In both cases, data were collected in 2 mm path length cells, and the CD baseline (only water in the cell) was subtracted. The data reported by the Aviv 60 apparatus, ellipticity (θ), were converted to $\Delta\varepsilon \equiv \varepsilon_L - \varepsilon_R$ (the difference in extinction coefficients for left and right circularly polarized light) for comparison with the results of the TRCD method. The experimentally measured quantity in the TRCD method is S, as defined by

$$S = (I_R - I_L)/(I_R + I_L)$$

where I_R is the intensity measured along the ellipse short axis after right elliptically polarized light traverses the sample and I_L is the analogous measurement with left elliptically polarized light.

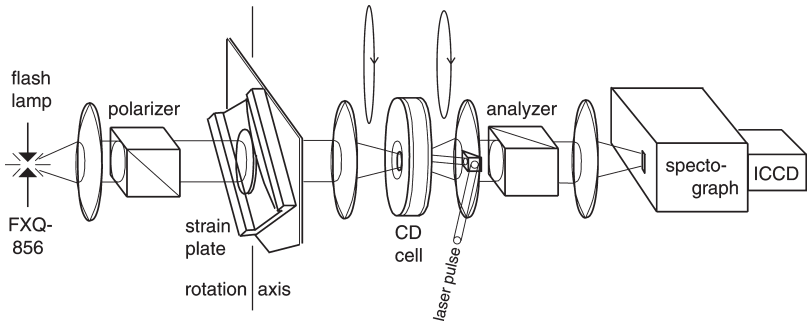

FIGURE 1: Apparatus for ellipsometric measurement of laser-induced circular dichroism change. White light from a short arc flash lamp is vertically polarized and then right elliptically polarized by the ~1° retardation of the strain plate in the orientation shown. Circular dichroism in the sample changes the short axis of the ellipse transmitted by the analyzer (a second linear polarizer crossed with respect to the first one). After dispersion of the white light in a spectrograph and at the desired delay following laser excitation, the wavelength dependence of the short axis intensity is detected by a gated intensified charge-coupled device (ICCD) detector (Andor IStar DK720). To compensate for other optical properties that can also affect the intensity along the short ellipse axis, we determined CD using measurements with right (as shown) and left (strain plate rotated 180° around the rotation axis) elliptically polarized light. In this figure, the ellipticity of the probe beam light before and after a sample displaying positive circular dichroism is shown using standard sectional patterns. The proportions of the ellipses were chosen for ease of display, with the actual ellipticities used here being approximately 10 times greater. Further details of the apparatus are given in ref *12*.

This is related to $\Delta\varepsilon$ by the following expression (*11*):

$$\Delta\varepsilon(\lambda) = \delta(\lambda)S/(2.3cl)$$

where $\delta(\lambda)$ is the wavelength-dependent retardation of the strain plate in radians, c is the concentration of rhodopsin, and l is the path length. The retardation of the fused silica plate used here was 1° at 550 nm, and the most significant change in that value with wavelength is due to the $1/\lambda$ dependence that arises from the fixed time retardation of a nondispersive plate translating into a larger fraction of a wave at shorter wavelengths (i.e., if there were no change in refractive index with wavelength, light at all wavelengths would be retarded by exactly the same time, but there will still be an $\sim 1/\lambda$ dependence to the phase angle retardation of the strain plate because the period of shorter wavelength waves is a shorter time). The dispersion of the stress optic coefficient in fused silica contributes much less to the $\delta(\lambda)$ wavelength dependence (*13*), and that effect was negligible here. The same procedure was used to convert the time-resolved CD measurements of rhodopsin photointermediates into $\Delta\varepsilon(\lambda)$. Results for static measurements obtained with the Aviv 60 and TRCD systems agreed within experimental uncertainty over the wavelength range of 300−700 nm.

RESULTS

Figure 2 shows the results obtained here for the static CD spectrum of rhodopsin in 4% lauryl maltoside. Two bands are present in the visible and near-UV portions of the spectrum, the α band, near the rhodopsin visible absorption maximum of 500 nm, and the much stronger rotational strength β band, near 340 nm where the so-called "cis" band appears in absorbance. Agreement was generally good between the results obtained using the ellipsometric TRCD apparatus and those obtained using a conventional CD instrument (Aviv 60). The rotational strengths of both the α and β bands in Figure 2 are smaller than those obtained by Okada et al. (*14*) at 5 °C using 0.6% CHAPS detergent and 0.8 mg/mL phosphatidylcholine to solubilize rhodopsin, but the circular dichroism spectrum of solubilized rhodopsin is known to depend both on the detergent used for solubilization and on the amount used (i.e., the final detergent:rhodopsin ratio) (*15*). At a lower detergent:rhodopsin ratio, we found the bands' rotational strength ratio, α/β, increased (data not shown) which is in general agreement with the effect of reduced detergent concentration on the rhodopsin CD spectrum seen by others.

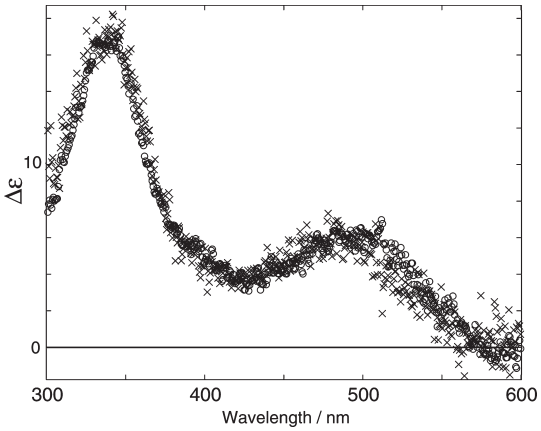

FIGURE 2: Circular dichroism of rhodopsin in 4% lauryl maltoside. Data obtained from measurement of a 1.7 mg/mL rhodopsin solution in a 2 mm path length cuvette using an Aviv 60 circular dichrograph (photoelastic modulator based) (○) and the TRCD apparatus shown in Figure 1 (×).

The signal changes measured at the three time delays after rhodopsin photoexcitation using the TRCD apparatus are shown in Figure 3. Five microseconds after photoexcitation, the primary photoproduct present is the first form of lumirhodopsin, Lumi I. The details of the small absorbance change associated with the Lumi I to Lumi II process have been determined previously for detergent suspensions at this temperature (*3*), and the general presence of lumirhodopsin was verified here from absorbance difference spectra calculated from a different combination of the data that were collected for CD determination. The two forms of lumirhodopsin have very similar absorption spectra (differing by only 2 nm) peaking near 490 nm and are the last protonated Schiff base photointermediates seen before the final deprotonated SB, G protein-activating form, Meta II, appears.

The raw data shown in Figure 3 are difference spectra produced by the photointermediates present minus the spectrum of the rhodopsin that disappeared to produce it. To determine absolute CD spectra of the photointermediates, the amount of rhodopsin bleached had to be determined and the appropriate CD added back. This was done by fitting the bleach of the

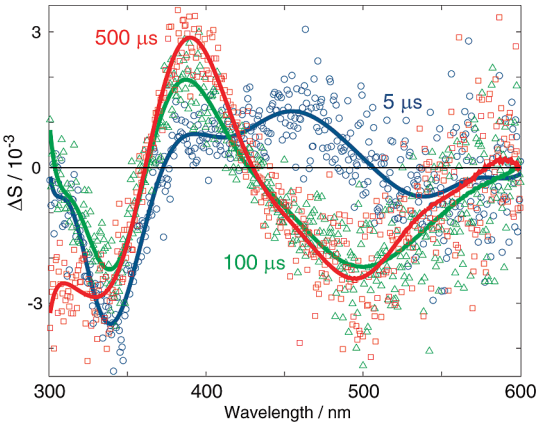

FIGURE 3: TRCD apparatus signal change after photoexcitation of rhodopsin in 4% lauryl maltoside. Data obtained at room temperature from measurements using a 1.7 mg/mL rhodopsin sample in a nominally 2 mm path length flow cuvette using the TRCD apparatus shown in Figure 1 with a gate delay of 5 (○), 100 (△), and 500 μs (□). Data points represent the change in the TRCD signal, *S*, between that observed at the time delay after the photoexcitation pulse noted and that observed immediately prior to the laser pulse with unphotolyzed rhodopsin present in the cuvette. Curves (shown in colors corresponding to the data points) were fit using polynomials and are presented as a visual aid.

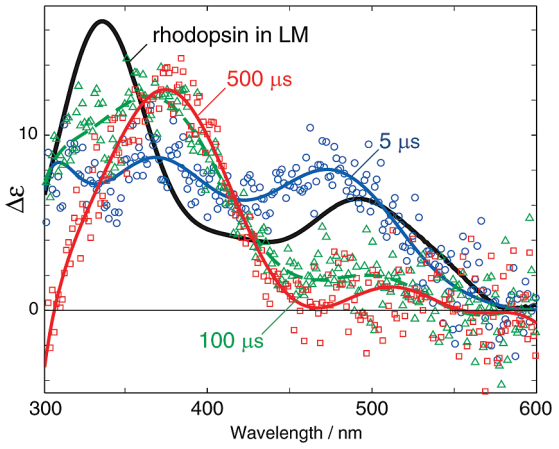

FIGURE 4: Absolute circular dichroism spectra observed after photoexcitation of rhodopsin in 4% lauryl maltoside. The data collected after photoexcitation (shown in Figure 3) were converted to the Δε form by correcting for the wavelength dependence of the strain plate retardation, δ (as described in Materials and Methods), and the measured circular dichroism spectrum of the bleached rhodopsin was added to the resulting data to produce absolute (photointermediates only) circular dichroism spectra at the delay times measured. To improve clarity, pairs of adjacent data points in Figure 3 were averaged to provide a single data point here. Blue circles represent data collected with a delay after photoexcitation of 5 μs (lumirhodopsin), green triangles data collected at 100 μs (equilibrated mixture of lumirhodopsin and Meta I_{380}), and red squares data collected at 500 μs (Meta II). Curves in corresponding colors (dashed in the case of the mixture) were fit using polynomials. The black curve shows the polynomial fit to the data, shown in Figure 2, collected using the conventional Aviv circular dichrograph. Curves fit to the data are provided to guide the eye, and small features that occur in them may not represent real bands; e.g., the 510 nm band in the Meta II curve is probably within the noise level of the data.

absorbance data calculated using a different combination of the data collected for CD experiment. For the measurements reported here, a bleach of 42% was estimated, which is generally consistent with previous measurements under these conditions. The absolute CD spectrum of lumirhodopsin (after correction for the bleach and the wavelength dependence of δ) is shown in Figure 4. Five microseconds after photoexcitation, the main changes that take place in the CD spectrum are a reduction in strength in the β band region and a blue shift of the α band (similar to that seen in the absorbance of lumirhodopsin relative to rhodopsin).

TRCD data obtained with a delay after photoexcitation of 100 μs represent a mixture composed of 57% lumirhodopsin and 43% Meta I_{380}, a deprotonated SB intermediate that appears in a transient equilibrium with lumirhodopsin before the later, stable deprotonated Meta II photointermediate forms. Although an absolute CD spectrum of the equilibrated mixture can be constructed by adding back the CD spectrum of 42% of the rhodopsin initially present, decomposition of the resulting absolute spectrum (see Figure 4) into CD spectra of its component species requires assumptions to be made, and the most natural one, i.e., that the CD spectrum of lumirhodopsin in the mixture is the same as that shown by the 5 μs curve in Figure 4, is invalid over at least part of the spectral range (see Discussion). At a delay of 500 μs, the sample again contains a single photointermediate, Meta II, and its absolute CD spectrum (Figure 4) was determined by adding back the CD spectrum of the 42% of the rhodopsin that was bleached to form it.

DISCUSSION

Several characteristic structural features of biopolymers specifically affect the polarization state of light. For example, a group of molecules with a particular orientation can be selected with an absorbed pulse of linear polarized light, allowing their subsequent rotation to be observed by measurement on an appropriate time scale with linearly polarized light. As another example, circularly polarized light has long been used as a tool to probe chiral structures in biopolymers, most frequently in the far-UV region to report on their secondary structure, but has also proven to be useful as a probe of the chiral environment of achiral amino acid side chains. Here we use time-resolved circular dichroism to study changes in the induced chirality of a prosthetic chromophore, the *N*-retinylidene Schiff base of rhodopsin, as the protein goes from the inactive, antagonist-bound form to the active form. Recent advances in the computation of rhodopsin's retinylidene chromophore CD, based on the X-ray crystal structure, provide an improved basis for the interpretation of these results (*16*).

CD measurements on the time scale we report are rare because photoelastic modulators, the standard tool used to elevate inherently small circular dichroism signals above noise, cannot be used in the submillisecond region. Instead, we use an alternative technique based on the 19th century observation that CD causes ellipticity changes in eliptically polarized light. Our method is implemented using modern technology, including an extremely bright source of white light, an optimized microretarder (*17*), and an ICCD gated array detector. A similar ellipticity-based technique has recently been applied successfully to CD measurements on an even faster time scale (*18*), but that method does not appear to be directly applicable in the presence of large absorbance changes, as is the case for the rhodopsin photochemistry studied here.

The ellipticity of polarized light is even more sensitive to linear birefringence than it is to circular dichroism which has the potential to cause serious artifacts in time-resolved CD measurements (*10*).

Nanosecond laser excitation of samples with linearly polarized light photoselects an oriented population of molecules that display linear dichroism until they either return to the original state or completely relax rotationally. Linear birefringence is always associated with linear dichroism (*19*), and both persist after photoexcitation of rhodopsin until complete rotational relaxation takes place. In its native membrane environment, rotational relaxation of rhodopsin takes approximately 10 μs (*20*) as measured with light propagating normal to the membrane, but the time scale of linear dichroism extends to times longer than the in-membrane rotational relaxation time when measurements are conducted in randomly oriented membrane suspensions (our unpublished results). The persistence of linear dichroism beyond the in-membrane rotational relaxation time in solution suspensions results from the need for membranes whose normal lies along the laser propagation direction to reorient to eliminate linear dichroism when probed by light propagating in the membrane plane (see ref *21*). The small size of the CD signal dictates that extensive signal averaging be done, which requires flow to remove the products of rhodopsin's irreversible photochemistry, so fast CD must be studied in some kind of suspension that allows complete rotational relaxation on the time scale preceding the CD measurement. Fortunately, the important photointermediates of rhodopsin, i.e., those involved in activation, also occur in detergent suspensions where complete rotational diffusion of rhodopsin has a submicrosecond time constant, and that is the state of rhodopsin characterized here.

TRCD of Rhodopsin Photointermediates versus Temperature-Trapped Results. Rhodopsin photointermediates have previously been studied using low-temperature trapping, which stabilizes some photointermediates sufficiently for characterization using conventional circular dichrographs. The CD spectrum obtained from lumirhodopsin trapped at −76 °C by Ebrey and Yoshizawa (*22*) agrees qualitatively with the result with a 5 μs delay reported here in Figure 4. Both the low-temperature trapped lumirhodopsin CD spectrum and the room-temperature 5 μs data show an ∼15 nm blue shift (compared to rhodopsin) of the α band in the visible and ∼50% reduction in the rotational strength of the near-ultraviolet β band (∼335 nm). The main quantitative difference between the previous low-temperature results and the room-temperature time-resolved result reported here concerns the rotational strength of the α band which was found to increase slightly here (compared to rhodopsin's α band) versus a small decrease that was found in the low-temperature trapped species. Agreement between the low-temperature and room-temperature time-resolved data is good considering the uncertainty in both experiments and the fact that solution conditions differed (for low-temperature trapping, the detergent was 1.5% Ammonyx LO and 1 part rhodopsin sample was mixed with 3 parts glycerol). Small amounts of isorhodopsin (< 10%), present in both experiments, were neglected.

The reduced rotational strength of the β band is the most pronounced difference seen between the CD spectrum of lumirhodopsin at 5 μs and that of the unphotolyzed pigment. A series of artificial visual pigments made from synthetic retinal analogues containing a second ring of various sizes connecting the retinal C5 ring methyl to C8 on the polyene chain suggest an explanation for this observation. When the added ring size was varied from five to eight carbons, the rotational strength of the resulting artificial pigment's β band decreased (*23*). The reduction in the β band was greatest in bicyclic model compounds with the largest added ring size, suggesting that reduction of the β band strength is associated with rotation of the C6−C7 single bond to open it away from the native 6*s*-*cis* geometry. This is an attractive explanation for the reduced β band rotational strength in lumirhodopsin since rotation of the retinal C6−C7 single bond has been previously suggested to account for the absorbance changes occurring during formation of the BSI photointermediate which immediately precedes lumirhodopsin (*6*).

The other photointermediate studied here that can be stabilized at low temperature is metarhodopsin II. The time-resolved results we report for metarhodopsin II are also in qualitative agreement with previous measurements for metarhodopsin II in this wavelength range. In agreement with Okada et al. (*14*), for metarhodopsin II we find a positive band with somewhat greater rotational strength compared to the α band of rhodopsin, centered near 380 nm which then switches sign near 300 nm to become negative at shorter wavelengths. The rotational strength of the band seen in time-resolved measurements here for metarhodopsin II is somewhat larger than that found by Okada et al. (*14*); however, their solubilization conditions (0.75% CHAPS and 1 mg/mL PC at 5 °C) were different from what we used, and consequently, their spectrum was for a mixture of metarhodopsin I and metarhodopsin II which would result in a reduced rotational strength for the metarhodopsin II portion of the band.

Lumirhodopsin CD Evolves over Time. After lumirhodopsin forms on the submicrosecond time scale, it partially decays in a detergent suspension to form Meta I_{380}, a species also seen after photoexcitation in the native membrane environment at higher temperatures (*9*). However, complete conversion of lumirhodopsin into Meta I_{380} does not take place even in detergent because a significant back-reaction from Meta I_{380} to lumirhodopsin causes an equilibrated mixture of the two species to form, which then subsequently decays to metarhodopsin II. The time-resolved CD measurement reported here at 100 μs characterizes the equilibrated mixture of approximately 60% lumirhodopsin and 40% Meta I_{380} (composition determined from time-resolved absorbance measurements). This is shown by the green triangle data points fit by the dashed curve in Figure 4. The result shown there is surprising because it suggests that the CD of the lumirhodopsin present in the equilibrated mixture has changed from the CD of the lumirhodopsin at 5 μs when it was initially formed. While absorbance measurements suggest that only ∼40% of the lumirhodopsin has decayed at 100 μs, the CD of the mixture has dropped by much more than that near the peak of the lumirhodopsin CD spectrum at 480 nm. This change in the CD measured in the visible range cannot result from the CD of Meta I_{380} in the mixture since Meta I_{380} does not absorb appreciably near 480 nm and hence does not contribute to the CD there. Thus, we must conclude that some process occurring between 5 and 100 μs dramatically reduces the lumirhodopsin α band CD. One possible candidate could be the evolution of the initially formed lumirhodopsin, Lumi I, into a second form, Lumi II, occurring with a lifetime of 13 μs and accompanied by a small absorbance change (*3*). In the measurements reported here, the time delays were selected primarily to characterize the Meta I_{380} species formed at later times, so determination of whether the CD change near 480 nm occurs on the same time scale as (and hence is associated with) the earlier Lumi I to Lumi II process will require further study at additional delay times. A second possible explanation for the reduction in the visible CD of lumirhodopsin at late times, after it forms an equilibrium with Meta I_{380}, is that the chirality of the chromophore changes in the

deprotonation−reprotonation process inherent in the equilibrium. This would suggest that some barrier between metastable rotational forms of the polyene is sensitive to the protonation state of the Schiff base so that the transition occurs more easily in the deprotonated state or during reprotonation. That would be interesting because SB deprotonation has been long associated with at least partial unlocking of rhodopsin's active state conformation (*24*−*26*). Further, chromophore conformational change in a structured polar environment such as that provided by the network of hydrogen bonds proposed to exist in the retinal binding pocket (*27*) could affect the SB p*K*, accounting for the back reprotonation seen in the lumirhodopsin to Meta I_{380} process, so a chirality change associated with initial Schiff base deprotonation would be an attractive explanation for the CD change seen here. In a twisted polyene structure, inversion of helicity could serve as a plausible trigger for protein change without necessarily being associated with a large shift in the absorbance spectrum.

CD of Meta I_{380}. The time evolution of the lumirhodopsin CD discussed above interferes with the original purpose of the TRCD measurements, i.e., to characterize whether the CD of Meta I_{380} differs from that of Meta II. The peak near 380 nm in the CD of the 100 μs equilibrated mixture certainly suggests that Meta I_{380} has a positive CD band, qualitatively similar to that of Meta II. However, without the ability to assume that the CD of lumirhodopsin in the mixture has the same CD spectrum as it did at 5 μs, it is impossible to make quantitative conclusions about the rotational strength of the Meta I_{380} band. If it is assumed that the CD of lumirhodopsin near 380 nm does not change in going from 5 to 100 μs (unlike the 480 nm CD which does change over this time range), we conclude that the $\Delta\varepsilon$ for Meta I_{380} is approximately 40% greater than the $\Delta\varepsilon$ is at 380 nm for Meta II. This would result in a quite large value for Meta I_{380}, larger than any band seen here, even in rhodopsin, which may suggest the chromophore in Meta I_{380} has the most extended helical twist of its double bonds. However, clarification of this point will require CD measurements at additional delay times and ultimately calculations on model structures.

Significance for the Rhodopsin Activation Mechanism. Since the advent of rhodopsin's X-ray crystal structure, circular dichroism studies have focused on far-UV characterization of changes in helix 8 upon activation (*28*). The helicity change that takes place in that amphipathic helix at the membrane surface, distant from the chromophore, must be one of the final steps in activation, and ideally, a continuous circular dichroism time record could describe the timing of that event relative to the chromophore changes we see here. Although time-resolved UV−TRCD measurements on the time scale required have been performed on some systems, in those cases extensive signal averaging was possible because the photochemistry was reversible. Extension of our measurements to the UV will require refinement of the current CD apparatus, or use of the complementary ORD property. A more serious limitation to direct extension of the work here is that rhodopsin helix 8 changes upon activation take place in only a membrane environment. However, nanodisks and nanoscale apolipoprotein-bound bilayer particles incorporating rhodopsin (*29*) may provide an ideal vehicle for such measurements.

Solid state NMR measurements have already provided some structural information about the chromophore in a thermally trapped form of Meta II. Those results suggest an elongation of the chromophore that moves the β-ionone ring several angstroms toward transmembrane helix 5 (*30*) and that the 13-methyl reorients to reduce chromophore torsion (*31*). The suggestion here that Meta I_{380} has a significantly greater CD than Meta II and hence retains more torsional strain is consistent with the idea that the changes seen in Meta II by NMR are either partially or wholly absent in the intitially deprotonated Meta I_{380}.

REFERENCES

1. Lewis, J. W., and Kliger, D. S. (2000) Absorption spectroscopy in studies of visual pigments: Spectral and kinetic characterization of intermediates. *Methods Enzymol. 315*, 164–178.
2. Jäger, S., Szundi, I., Lewis, J. W., Mah, T. L., and Kliger, D. S. (1998) Effects of pH on rhodopsin photointermediates from lumirhodopsin to metarhodopsin II. *Biochemistry 37*, 6998–7005.
3. Szundi, I., Lewis, J. W., and Kliger, D. S. (2003) Two intermediates appear on the lumirhodopsin time scale after rhodopsin photoexcitation. *Biochemistry 42*, 5091–5098.
4. Palings, I., Pardoen, J. A., Vandenberg, E., Winkel, C., Lugtenburg, J., and Mathies, R. A. (1987) Assignment of fingerprint vibrations in the resonance raman-spectra of rhodopsin, isorhodopsin, and bathorhodopsin: Implications for chromophore structure and environment. *Biochemistry 26*, 2544–2556.
5. Birge, R. R., Einterz, C. M., Knapp, H. M., and Murray, L. P. (1988) The nature of the primary photochemical events in rhodopsin and isorhodopsin. *Biophys. J. 53*, 367–385.
6. Lewis, J. W., Fan, G.-B., Sheves, M., Szundi, I., and Kliger, D. S. (2001) Steric barrier to bathorhodopsin decay in 5-demethyl and mesityl analogues of rhodopsin. *J. Am. Chem. Soc. 123*, 10024–10029.
7. Arnis, S., and Hofmann, K. P. (1993) Two different forms of metarhodopsin-II: Schiff-base deprotonation precedes proton uptake and signaling state. *Proc. Natl. Acad. Sci. U.S.A. 90*, 7849–7853.
8. Knierim, B., Hofmann, K. P., Ernst, O. P., and Hubbell, W. L. (2007) Sequence of late molecular events in the activation of rhodopsin. *Proc. Natl. Acad. Sci. U.S.A. 104*, 20290–20295.
9. Thorgeirsson, T. E., Lewis, J. W., Wallace-Williams, S. E., and Kliger, D. S. (1993) Effects of temperature on rhodopsin photointermediates from lumirhodopsin to metarhodopsin-II. *Biochemistry 32*, 13861–13872.
10. Einterz, C. M., Lewis, J. W., Milder, S. J., and Kliger, D. S. (1985) Birefringence effects in transient circular-dichroism measurements with applications to the photolysis of carbonmonoxyhemoglobin and carbonmonoxymyoglobin. *J. Phys. Chem. 89*, 3845–3853.
11. Lewis, J. W., Tilton, R. F., Einterz, C. M., Milder, S. J., Kuntz, I. D., and Kliger, D. S. (1985) New technique for measuring circular dichroism changes on a nanosecond time scale. Applications to (carbonmonoxy) myoglobin and (carbonmonoxy) hemoglobin. *J. Phys. Chem. 89*, 289–294.
12. Lewis, J. W., Gu-Thomas, Y., and Kliger, D. S. (2007) Time-resolved circular dichroism as a structural probe of rhodopsin photolysis intermediates. In Methods in Protein Structure and Stability Analysis: Luminescence Spectroscopy and Circular Dichroism (Uversky, V. N., and Permyakov, E. A., Eds.) pp 345−356, Nova Science Publishers, Inc., New York.
13. Vasudevan, T. N., and Krishnan, R. S. (1972) Dispersion of the stress-optic coefficient in glasses. *J. Phys. D: Appl. Phys. 5*, 2283–2287.
14. Okada, T., Matsuda, T., Kandori, H., Fukada, Y., Yoshizawa, T., and Shichida, Y. (1994) Circular dichroism of metaiodopsin II and its binding to transducin: A comparative study between Meta II intermediates of iodopsin and rhodopsin. *Biochemistry 33*, 4940–4946.
15. Wagner, J., Smith, E., and Cusanovich, M. A. (1981) The circular dichroism of sodium cholate solubilized rhodopsin. *Photochem. Photobiol. 33*, 929–932.
16. Pescitelli, G., Sreerama, N., Salvadori, P., Nakanishi, K., Berova, N., and Woody, R. W. (2008) Inherent chirality dominates the visible/near-ultraviolet CD spectrum of rhodopsin. *J. Am. Chem. Soc. 130*, 6170–6181.
17. Esquerra, R. M., Lewis, J. W., and Kliger, D. S. (1997) An improved linear retarder for time-resolved circular dichroism studies. *Rev. Sci. Instrum. 68*, 1372–1376.
18. Hache, F. (2009) Application of time-resolved circular dichroism to the study of conformational changes in photochemical and photobiological processes. *J. Photochem. Photobiol., A 204*, 137–143.
19. Christy, R. W. (1972) Classical theory of optical dispersion. *Am. J. Phys. 40*, 1403–1419.
20. Cone, R. A. (1972) Rotational diffusion of rhodopsin in visual receptor membrane. *Nat. New Biol. 236*, 39–43.

21. Cherry, R. J., and Godfrey, R. E. (1981) Anisotropic rotation of bacteriorhodopsin in lipid-membranes: Comparison of theory with experiment. *Biophys. J. 36*, 257–276.
22. Ebrey, T. G., and Yoshizawa, T. (1973) The circular dichroism of rhodopsin and lumirhodopsin. *Exp. Eye Res. 17*, 545–556.
23. Wada, A., Tsutsumi, M., Inatomi, Y., Imai, H., Shichida, Y., and Ito, M. (2001) Retinoids and related compounds. Part 26.1 Synthesis of (11Z)-8,18-propano- and methano-retinals and conformational study of the rhodopsin chromophore. *J. Chem. Soc., Perkin Trans. 1,* 2430–2439.
24. Longstaff, C., Calhoon, R. D., and Rando, R. R. (1986) Deprotonation of the Schiff-base of rhodopsin is obligate in the activation of the G-protein. *Proc. Natl. Acad. Sci. U.S.A. 83*, 4209–4213.
25. Cohen, G. B., Oprian, D. D., and Robinson, P. R. (1992) Mechanism of activation and inactivation of opsin: Role of Glu(113) and Lys-(296). *Biochemistry 31*, 12592–12601.
26. Zvyaga, T. A., Fahmy, K., and Sakmar, T. P. (1994) Characterization of rhodopsin-transducin interaction: A mutant rhodopsin photoproduct with a protonated Schiff-base activates transducin. *Biochemistry 33*, 9753–9761.
27. Ahuja, S., Hornak, V., Yan, E. C. Y., Syrett, N., Goncalves, J. A., Hirshfeld, A., Ziliox, M., Sakmar, T. P., Sheves, M., Reeves, P. J., Smith, S. O., and Eilers, M. (2009) Helix movement is coupled to displacement of the second extracellular loop in rhodopsin activation. *Nat. Struct. Mol. Biol. 16*, 168–175.
28. Krishna, A. G., Menon, S. T., Terry, T. J., and Sakmar, T. P. (2002) Evidence that helix 8 of rhodopsin acts as a membrane-dependent conformational switch. *Biochemistry 41*, 8298–8309.
29. Banerjee, S., Huber, T., and Sakmar, T. P. (2008) Rapid incorporation of functional rhodopsin into nanoscale apolipoprotein bound bilayer (NABB) particles. *J. Mol. Biol. 377*, 1067–1081.
30. Patel, A. B., Crocker, E., Eilers, M., Hirshfeld, A., Sheves, M., and Smith, S. O. (2004) Coupling of retinal isomerization to the activation of rhodopsin. *Proc. Natl. Acad. Sci. U.S.A. 101*, 10048–10053.
31. Ahuja, S., Crocker, E., Eilers, M., Hornak, V., Hirshfeld, A., Ziliox, M., Syrett, N., Reeves, P. J., Khorana, H. G., Sheves, M., and Smith, S. O. (2009) Location of the retinal chromophore in the activated state of rhodopsin. *J. Biol. Chem. 284*, 10190–10201.